

Infrared absorption in oxides in the presence of both large and small polarons

David M. Eagles,* Ricardo P. S. M. Lobo, and François Gervais†

Centre de Recherches sur la Physique des Hautes Températures, CNRS, 45071 Orléans Cedex 2, France

(Received 29 November 1994; revised manuscript received 19 May 1995)

Infrared conductivity in oxides when two types of polaron are present is discussed, and experiments on $\text{Pr}_2\text{NiO}_{4.22}$ in the *ab* plane are analyzed in detail. Infrared reflectivity spectra on a crystal of this material between 30 and 20000 cm^{-1} have been obtained from 77 K up to room temperature. The low-energy region (up to 1000 cm^{-1}) can be interpreted as phonon spectra screened by a plasmon. Thermal evolution of the screening of phonons shows the semiconducting behavior of this material. Conductivity data obtained from Kramers-Kronig transformations for frequencies between 1000 and 16000 cm^{-1} are fitted by a theory involving the simultaneous presence of large and small polarons. Due to expectations of relatively large effects of disorder and of Coulomb interactions on properties of large polarons, one contribution to the absorption, that for which the initial and final state is in the wide (large-polaron) band, is approximated as a Gaussian with adjustable center position and width. The other three contributions, involving at least one of the initial or final states in the narrow (small-polaron) band are treated by modifications of previously published theories for small concentrations of polarons. In all there are seven parameters in the theory. After preliminary fits in which each parameter is treated as adjustable at each temperature, the phonon energy was fixed at 0.064 eV, with the other parameters determined by fitting. The fits are approximately as good as the estimated accuracy of the conductivity data, and the fitted values occur in ranges expected from the theory. Values of parameters associated with small polarons imply a large contribution to binding energies from short-range forces. Combining results for parameters with the conductivity data of Allançon *et al.* enables estimates to be made of the approximate position of the mobility edge in the wide band and of orders of magnitude of concentrations of mobile carriers. Plasma frequencies are inferred to be very low below room temperature, and highly temperature dependent.

I. INTRODUCTION

There is considerable controversy about interpretation of infrared absorption data in both superconducting and nonsuperconducting oxides.¹ In the cuprates models used have included: (i) A Drude term with a frequency-dependent effective mass and a frequency-dependent damping constant,² (ii) a Drude term plus a midinfrared band due to (a) large polarons,³ (b) small polarons,⁴ (c) bipolarons,⁵ or (d) to transitions involving localized states,⁶ and (iii) theories based on models such as the *t*-*J* model in which effects of strong correlations are dominant.⁷ For other oxides there have not been quite so many types of theories put forward, but there are still differing interpretations. In some oxides the main question is what type of polaron theory is required, e.g., SrTiO_3 ,^{8,9} whereas in other oxides besides the cuprates it is not generally agreed upon whether polaron theory is applicable, e.g., $(\text{La,Sr})_2\text{NiO}_4$.¹⁰⁻¹² We think that in some cases the disagreement about the type of polaron theory to use in a particular material may arise because of the simultaneous presence of two types of polaron, either as almost independent species or with significant mixing of the states associated with each type.

It was shown previously¹³ that it is possible that in some materials the conditions of validity for large-polaron theory and for what we call nearly-small-polaron theory can both be satisfied at the same time. Since the two types of polaron wave functions are not orthogonal,

and have nonzero matrix elements of the Hamiltonian between them, the lowest state of the system is composed of a mixture of large and nearly small polarons, with ground- and excited-state mixtures at any given wave vector.¹⁴⁻¹⁶

While the conditions for a superposition of the two types of polaron to be a good approximation to the true state of the system were not examined in Refs. 14-16, the work of Lépine and Frongillo¹⁷ sheds some light on this problem. These authors perform calculations for a tight-binding model on a simple-cubic lattice with a Fröhlich type of electron-phonon interaction,¹⁸ for various values of the ratio to the phonon energy ω of the modulus J of the matrix element of the one-electron Hamiltonian between local states on near-neighbor atoms; J can be referred to briefly as an electronic transfer integral. For $6J = \omega$ the variational method of Ref. 17 gives quite gradual changes of polaron properties as a function of the coupling constant α , for $6J = 2\omega$ the changes are sharp near $\alpha = 3$, and for $6J = 5\omega$ they find two types of solutions for a range of α between about 2.7 and 4.7, one resembling a small polaron and the other a large polaron, with a crossover of the stable state at $\alpha \sim 3.7$. Presumably a more general variational method allowing mixtures of the two types would prevent the transition from being discontinuous, and so, for values of J which are not too small, there appears to be a range of coupling constants for which the type of wave function which was used in Refs. 9 and 14-16 is a reasonable approximation.

A theory for optical absorption by mixed polarons was developed in Ref. 15. There are four types of contribution to the absorption in this theory, according to whether the wide- or narrow-band components of the initial and final states are involved. Three of the components were treated by methods similar to those published over 30 years ago,¹⁹ but with expressions put in terms of electronic transfer integrals as in the formulation of Reik⁸ for small polarons rather than in terms of matrix elements of the gradient operator as in Ref. 19. The fourth contribution was treated by a weak-coupling formalism analogous to that used by Devreese, Huybrechts, and Lemmens²⁰ for large polarons in the weak-coupling limit.

Alexandrov, Kabanov, and Ray²¹ have used numerical methods on small clusters to study optical absorption in intermediate- and strong-coupling regimes for a model with short-range interactions, and find departures from predictions of small-polaron theory for intermediate coupling. However we do not see much obvious similarity to what we expect in our model. Possibly the use of small clusters results in a gradual transition between polaron types even for overlap integrals larger than phonon frequencies in contrast to what can be expected in the bulk for large transfer integrals. We conjecture that this is the cause of differences between predictions of Ref. 21 and of our model. The theory of Ref. 15 was applied to SrTiO₃ in Ref. 9.

The discovery of superconductivity in copper-lanthanum oxides by Bednorz and Müller²² has attracted great interest in the nickel-based family $L_2\text{NiO}_{4+\delta}$, L being a rare earth (La, Pr, Nd). Praseodimium compounds, particularly, have several phase transitions (magnetic, structural, and electronic^{23–25}) either as a function of temperature or of oxygen stoichiometry. Even if high- T_c superconductivity is not present in these nickel-based compounds, the possibility of obtaining large single crystals makes these materials very attractive for spectroscopic measurements. Comparing nickelates and cuprates is also interesting for understanding normal-state conductivity. The properties of these materials are strongly influenced by the layered structure, with many properties depending only on properties of the Ni-O planes. In our theory the layered structure comes in only via the number of non-negligible electronic transfer integrals and by an assumption we make of a rectangular density of states for the wider of two bands appearing in our theory.

An extremely powerful tool to analyze these materials is infrared spectroscopy. Infrared reflection on conducting materials allows us to obtain information basically on four different responses to the dielectric function: phonons, plasmon, an eventual superconducting gap, and midinfrared excitations. Some infrared experiments and discussion of results for two different compositions of $\text{Pr}_2\text{NiO}_{4+\delta}$ have been published previously.^{26,27}

Bi, Eklund, and Honig^{10,11} have analyzed a midinfrared absorption band in $\text{La}_{2-x}\text{Sr}_x\text{NiO}_{4+\delta}$ with the theory of optical absorption by small polarons,^{8,19} using the form of expressions for this given by Reik,⁸ which can be shown to be equivalent to expressions given earlier in Ref. 19. They obtain a good fit to data for photon ener-

gies between 0.1 and 0.4 or 0.5 eV using plausible values of parameters, except perhaps for a rather small value for the electronic transfer integral, $J=0.08$ eV. However, at higher photon energies there is not even a qualitative similarity with experiment.

Crandles *et al.*¹² have given three possible further objections related to (i) the disagreement with observed activation energies for dc conductivity with those deduced from optical data, (ii) the low phonon frequencies needed to fit the observed temperature dependence, and (iii) the lack of an observed shift of oscillator strength from low to higher frequencies as the temperature is decreased.

We think that, in principle, objection (i) could be overcome by supposing that the activation energy for dc conductivity when J is large compared with the photon energy is reduced by J , and that this reduction becomes less as J approaches the phonon energy from above. The potential energy at the saddle point in an adiabatic theory of small polarons has such a reduction by J .^{28,13} However we think, for reasons which will be explained later, that, at least in $\text{Pr}_2\text{NiO}_{4.22}$, the activation energy for dc conduction is dominated by activation of current carriers other than small polarons to a mobility edge. Objection (ii) may be connected with the inadequacy of a model with a single phonon energy to describe all features of the absorption. Because of Bose factors, the temperature dependence at low frequencies will be dominated by low-energy phonons even if the coupling to these is relatively weak, as expected for long-range forces when there are several longitudinal polar modes,²⁹ whereas the overall shape will be determined by an average frequency weighted by coupling strengths. However, objection (iii) and the lack of agreement with experiment at photon energies greater than about 0.5 eV point to the necessity of a more complex model. In this paper we use a model involving the simultaneous presence of two types of polaron to interpret data on $\text{Pr}_2\text{NiO}_{4.22}$.

We have measured the thermal dependence (from 77 K to room temperature) of infrared reflection of the ab plane of $\text{Pr}_2\text{NiO}_{4.22}$ in a spectral range of 30 to 20 000 cm^{-1} . Measurements along the c axis have already been done and show insulating behavior.²⁶ The spectra obtained clearly show contributions of three different excitations: phonons, almost temperature independent midinfrared bands, and a thermally activated response of free charges. Phonon behavior can be understood in the framework of the commonly used oscillatorlike model. Higher energy (midinfrared) conductivity data (obtained by Kramers-Kronig transformation of reflectivity spectra) can be explained by a model involving the simultaneous presence of two types of polaron.

Experimental results are presented in Sec. II, and fitted in Secs. III and IV with conventional models in the low-frequency range and with a model involving both small and large polarons at frequencies between 1000 and 16 000 cm^{-1} . A discussion of the fits is given in Sec. V.

II. EXPERIMENTAL RESULTS

A $\text{Pr}_2\text{NiO}_{4.22}$ single crystal was obtained by annealing at 450 °C from a $\text{Pr}_2\text{NiO}_{4+\delta}$ crystal grown by K. Dembin-

ski by a zone-melting technique with a CO₂ laser in ambient atmosphere. This method assures that the ratio [Pr]/[Ni] is very close to 2. It has been described elsewhere.³⁰ Oxygen stoichiometry is obtained via thermogravimetric analysis. Infrared spectra have been obtained with a new Bruker IFS 307 Fourier spectrometer composed of two complementary interferometers covering spectral ranges of 8 to 15 000 cm⁻¹ and 3000 to 40 000 cm⁻¹. The cryostat has been equipped with polyethylene, thallium bromiodine, and Suprasil 300 windows in order to cover, respectively, far-infrared, mid-infrared and near-infrared-visible regions. Temperature accuracy of 0.5 K has been attained by means of a CTLS probe. Optical conductivity data have been determined by Kramers-Kronig (KK) transforms. Slightly different extrapolations to zero and high frequencies yield different behavior in KK-transform-obtained properties. In order to avoid this kind of problem, we kept out attention to data between 1000 and 16 000 cm⁻¹ as this region showed no dependence on the kind of extrapolation used. (Actually the low-frequency limit is about 50 cm⁻¹ but the region between 50 and 1000 cm⁻¹ is not interesting for our conductivity analysis.)

III. FITS TO DATA BELOW 1000 cm⁻¹

The low-frequency region of the infrared spectra can be fitted by a phonon model. From Maxwell's equations we know that transverse (TO) and longitudinal (LO) optical modes are, respectively, poles and zeros of the dielectric function. We can, thus, factorize the phonon contribution to the dielectric function in terms of the frequencies (ω) and dampings (γ) of these modes,³¹ giving

$$\epsilon_{\text{ph}} = \epsilon_{\infty} \prod_j \frac{\Omega_{j\text{LO}}^2 - \omega^2 + i\omega\gamma_{j\text{LO}}}{\Omega_{j\text{TO}}^2 - \omega^2 + i\omega\gamma_{j\text{TO}}}, \quad (1)$$

where ϵ_{∞} is the high-frequency dielectric constant. In order to take into account screening of phonons, a modified Drude-like contribution for the dielectric function has been used. In this model one can allow different values for damping (γ) at zero and plasma frequencies. This contribution for the dielectric function is written as

$$\epsilon_{\text{pl}} = -\epsilon_{\infty} \frac{\Omega_{\text{pl}}^2 + i(\gamma_{\text{pl}} - \gamma_0)}{\omega(\omega - i\gamma_0)}. \quad (2)$$

In our low-frequency fits, we took plasma frequencies which satisfied two conditions: (i) screening of the phonons should appear properly in fits and (ii) theoretically obtained conductivity just above the phonon region should match fits obtained with the microscopic model presented in this paper. However, we must emphasize that this plasma frequency is just an *ad hoc* parameter used to represent observed screening of phonons at low frequencies within the *ab* plane.

We present in Fig. 1 the reflectivity on the *ab* plane in the low-frequency region (up to 1000 cm⁻¹). Experimental data are represented by points and best fits using Eqs. (1) and (2) are solid lines. Comparing the data between 300 and 77 K we can clearly see the effect of thermally activated charge carriers in nickelates which had already

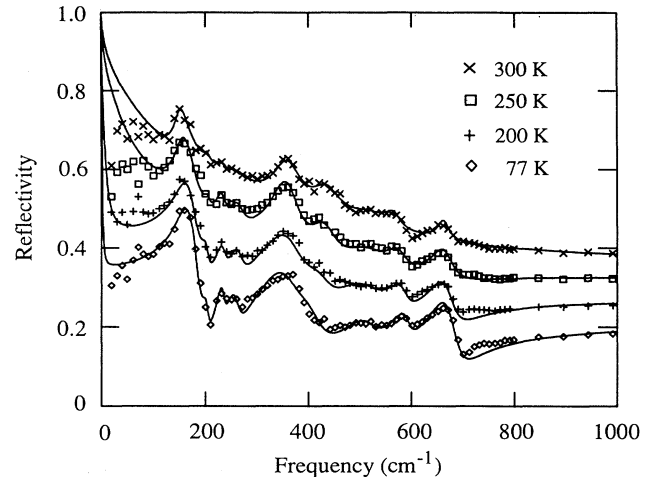


FIG. 1. *ab* plane reflectivity data (points) up to 1000 cm⁻¹ at temperatures from 77 K up to 300 K and fit (solid lines) with Eqs. (1) and (2).

been observed for lanthanum compounds.³¹ Basically no difference is observed in phonons of praseodymium- or lanthanum-based nickelates. *ab* plane and *c* axis infrared phonon behavior in these materials have already been the subject of some works.^{26,27,31}

IV. FITS TO DATA FROM 1000 TO 16 000 cm⁻¹ USING THEORY INVOLVING LARGE AND SMALL POLARONS

In this section we make use of a theory of optical absorption by mixed polarons developed in Ref. 15 to analyze the data of Sec. II. However we make the assumption (justified after parameters are determined) that the mixing is negligible, and hence the theory reduces to that for optical absorption when large and nearly small polarons lie close in energy, without mixing. As for the case when mixing occurs, if both types of polaron state are partially occupied, there are four types of contribution to the optical absorption, (i) $N \rightarrow N$, (ii) $W \rightarrow N$, (iii) $N \rightarrow W$, and (iv) $W \rightarrow W$, where N and W refer to narrow- and wide-band components of initial- and final-state wave functions. For the case of no mixing N and W just refer to states in the narrow band (small polarons) and the wide band (large polarons).

Since there will be a frequency dependence to the refractive index, n , and we do not have a theory for n for the model we are using, we analyze the real part of the conductivity rather than the absorption coefficient, which has a dependence on n . We denote the four contributions to the conductivity associated with the processes mentioned above by $\sigma_1(N \rightarrow N)$, $\sigma_2(W \rightarrow N)$, $\sigma_3(N \rightarrow W)$, and $\sigma_4(W \rightarrow W)$. For the first three contributions we make use of the theory of Ref. 15, specialized to the case of no mixing, and modified for non-negligible band filling. However, since preliminary analysis of data using the model indicated that the fourth contribution was much broader than expected according to the theory of absorp-

tion by small concentrations of large polarons,³² we treat σ_4 in a simpler manner by assuming it has a Gaussian form with an adjustable center frequency and width, with a strength such that the integrated absorption is approximately the same as calculated by Devreese, de Sitter, and Goovaerts³² for a large-polaron coupling constant $\alpha=3$. There are reports in the literature of effects of disorder and of Coulomb repulsion on optical absorption by small polarons,³³ but we are not aware of similar calculations for large polarons. However, it seems safe to say that both disorder and interactions will tend to broaden the absorption and shift its maximum to higher frequencies.

Our reason for assuming small mixing at the outset for $\text{Pr}_2\text{NiO}_{4.22}$ is that a plasma frequency which increases with increasing temperature has been reported in the related compound $\text{La}_2\text{NiO}_{4+8}$ (and is confirmed here as shown by the fit in Fig. 1) whereas if the mixing energy is larger than a quantity of the order of $k_B T$, the opposite temperature dependence can be expected. This occurs in SrTiO_3 ,³⁴ consistent with analysis¹⁶ of observed temperature dependences of masses in this material determined by other methods.³⁵

Although in the nickelates the current carriers are holes in the valence band, for our theoretical development we shall use terminology appropriate for electrons in a conduction band. When applying the theory to the nickelates we have to remember that changes of terminology are required, e.g., "above the bottom of the band" should be replaced by "below the top of the band."

Making the approximations that mixing of types of polarons and the width of the narrow band can be neglected, the contribution σ_1 to the conductivity due to $N \rightarrow N$ transitions can be found from Eqs. (12) to (17) of Ref. 15 with the following differences: (a) $1/2(1-\delta/\lambda)n_m$ in Eq. (12) is replaced by n_1 , the concentration of narrow-band polarons; (b) I_0 in Eq. (12) is put equal to zero because we are assuming negligible mixing; (c) a quantity ϵ in Eq. (17) of Ref. 15, giving the average separation between the bottom of the mixed polaron band and the average energy of the narrow band is replaced by zero here, since the transitions are from the narrow band to other states of the same band, and its band width is assumed to be negligible; (d) we introduce a factor $(1-0.5n_1\eta^{-1}V_a)$, where V_a is the volume per relevant atom (Ni here), and η is a possible degeneracy factor because of several types of d orbitals. We also multiply by an appropriate factor to convert from absorption coefficients to conductivity.

The expressions for absorption used in Ref. 15 involve a simple method of smoothing the set of δ -function peaks which would occur with no phonon or polaron dispersion into continuous curves which occur when dispersion is included. It was argued in Ref. 15 that the particular type of smoothing used was not important and errors due to the type used were estimated to be small. However the method used does have the drawback of giving discontinuous slopes of the conductivity at some photon energies, as opposed to the method of Reik⁸ for small polarons which does not have this problem, but gives slightly more complicated expressions to evaluate at intermediate temperatures.

In the same approximation of negligible mixing of polaron types, but with inclusion of effects of unavailability of some final states in a simplified way, calculations similar to that giving Eq. (19) of Ref. 15 can be used to find the contributions σ_2 and σ_3 to the conductivity due to $W \rightarrow N$ and $N \rightarrow W$ transitions for a rectangular density of states of width for the wide band assumed to be approximately equal to the bare bandwidth W_b , with occupation up to an energy E_F above the bottom of the band. Since the differences from expressions used in Ref. 15 are not so trivial for these contributions, especially for σ_2 , we write the expression used in more detail. We find

$$\sigma_2 = C(2V_a^{-1} - n_1\eta^{-1})(\omega/W_b)R(p, T, \delta), \quad (3)$$

and

$$\sigma_3 = Cn_1(\omega/W_b)Q(p, T, \delta). \quad (4)$$

Here, using electrostatic units for the conductivity,

$$C = \pi z \eta a^2 e^2 J^2 / 3 \hbar \omega^2, \quad (5)$$

where z is the number of nearest neighbors, η is the possible degeneracy factor mentioned before, a is the lattice constant, J is an electronic transfer integral between near-neighbor Ni atoms (for oxides this is indirect, via oxygens³⁶), and ω here denotes the phonon energy rather than the angular frequency as in Ref. 15; the other quantities in Eqs. (3) and (4) are

$$p = \Omega/\omega, \quad (6)$$

where Ω is the photon energy,

$$R = p^{-1} \left\{ \sum_{s=i_0}^{i_1} [H_2(s, \bar{n})] + r_1 H_2(i_1 + 1, \bar{n}) + r_0 H_2(i_0 - 1, \bar{n}) \right\} (E_F > \omega), \quad (7)$$

$$R = p^{-1} (E_F/\omega) [(r_1 H_2(i_1 + 1, \bar{n}) + r_0 H_2(i_0 - 1, \bar{n})) (E_F < \omega)], \quad (8)$$

and

$$Q = p^{-1} \left\{ \sum_{s=j_0}^{j_1} [H_2(s, \bar{n})] + q_1 H_2(j_1 + 1, \bar{n}) + q_0 H_2(j_0 - 1, \bar{n}) \right\}. \quad (9)$$

In these equations, H_2 is defined in Ref. 15, and depends on a parameter S_2 , the preferred number of photons to be emitted for $W \rightarrow N$ and $N \rightarrow W$ processes, \bar{n} is the phonon thermal occupation number, $\delta\omega$ is the energy position of the narrow band measured from the bottom of the wide band, i_1 is the largest (positive, negative or zero) integer smaller than $[(p - \delta - 0.5 + \max(E_F/\omega, 1)]$, j_1 is the largest (positive, negative or zero) integer smaller than $(p + \delta - 0.5 - E_F/\omega)$,

$$r_1 = p - \delta - 0.5 + \max(E_F/\omega, 1) - i_1, \quad (10)$$

$$q_1 = p + \delta - 0.5 - E_F/\omega - j_1, \quad (11)$$

i_0 is the smallest (positive, negative or zero) integer greater than $(p - \delta + 0.5)$, j_0 is the smallest (positive, negative or zero) integer greater than $(p + \delta + 0.5 - W_b/\omega)$,

$$r_0 = i_0 - p + \delta - 0.5, \quad (12)$$

and

$$q_0 = j_0 - p - \delta - 0.5 + W_b/\omega. \quad (13)$$

The expressions used here for σ_2 are different from those used in Ref. 15 since we are assuming a non-negligible width of the occupied part of the wide band, and so σ_2 has to be treated in a similar manner to σ_3 . Note also that the signs in front of δ appearing in Eqs. (11) and (13) and the related expressions for j_1 and j_0 are opposite to those in front of a quantity λ appearing in expressions after Eq. (21) of Ref. 15, because there we were considering transitions from the bottom of the lower mixed-polaron band to the upper mixed-polaron band, whereas here we are considering transitions from a state with energy $\delta\omega$ above the bottom of the wide band to the wide band. If $E_F < 2\omega$ it is possible for i_0 to be greater than i_1 , in which case the sum in Eq. (7) is taken to be zero.

The method of smoothing sharp jumps in absorption used in Ref. 15 when a process in which a net number n of phonons are emitted starts or stops because $(\Omega \pm \delta\omega - n\omega)$ passes through the band edges (or Fermi level here), involved replacing the step functions in the densities of states by linearly rising or falling densities of states spread over an energy ω to simulate the smoothing of absorption coefficients by dispersion of phonon frequencies. However, when $E_F < \omega$, this method is not applicable, and instead we have used an expression similar to that for $E_F = \omega$, but scaled down by a factor E_F/ω to account for the smaller carrier concentrations in the wide band for smaller E_F . Thus for $E_F < \omega$ we have expressions of a similar type to those for the $N \rightarrow N$ contribution to the conductivity.

The above expressions assume that E_F is positive and neglect temperature smearing of the Fermi distribution. The temperature smearing will give only a small broadening on the scale of the total widths of the two contributions to the conductivity. For $E_F < 0$, σ_2 can be treated by methods similar to those used for σ_1 as in Ref. 15, and in the same case of negative E_F an approximation for σ_3 would be to replace E_F by zero in the expressions for j_1 and q_1 , but instead multiply the right-hand side of Eq. (4) by a factor $(1 - 0.5n_2\eta^{-1}V_a)$, where n_2 is the concentration of wide-band carriers, in analogy to the factor $(1 - 0.5n_1\eta^{-1}V_a)$ which we used when calculating σ_1 .

For a simple cubic or square lattice the bare bandwidth is related to the electronic transfer integral J by $W_b = 2zJ$, where z is the number of near neighbors of a given atom. For $\text{Pr}_2\text{NiO}_{4.22}$ we shall approximate the Ni arrangement within a plane as square and ignore interplanar overlaps, giving $z = 4$.

Preliminary fits to the data for photon frequencies

greater than 5000 cm^{-1} using just the first three contributions to the conductivity indicated that the fourth contribution, due to $W \rightarrow W$ transitions, must be much broader and flatter than that given by the theory of optical absorption by large polarons,³² and so for this contribution we decided to use a very simple Gaussian form with an adjustable peak position and width, but with an integrated strength approximately that calculated by Devreese, de Sitter, and Goovaerts³² for a coupling constant $\alpha = 3$. The units used in Ref. 32 appears to be rather unusual, but we converted results from the figures there to more usual units by comparison with weak-coupling results.²⁰ The differences from the calculated results are assumed to come from disorder and Coulomb interactions, both of which can increase the position of maximum absorption and width in the case of small polarons.³³ The relative importance of these effects can be expected to be larger for a given concentration of large polarons than for the same concentration of small polarons since the initial position of the peak conductivity and width for a small concentration of large polarons is much smaller than for small polarons, at least until one gets to very strong large-polaron coupling constants when a simplified theory such as that of Emin³⁷ might become a fair approximation. Also large polarons will come closer to overlapping than small polarons for a given concentration, and so this give another reason for the probable greater effects of interactions for large polarons.

Thus we suppose that

$$\sigma_4 = 0.7(\xi n_2 e^2 \hbar / m_b \Gamma \pi^{1/2}) \exp[-(\Omega - E_0)/\Gamma]^2] \times (1 - 0.5n_2\eta^{-1}V_a). \quad (14)$$

Here m_b is the bare (band-structure) electron mass, E_0 and Γ are the center and halfwidth (for a fall by a factor e^{-1}) of a Gaussian to be determined by data fitting, ξ is a degeneracy factor for this type of transition which may be equal η or to 1 depending on details of the band structure,¹⁵ and the approximate numerical factor of 0.7 was obtained by making the integrated conductivity approximately the same as inferred from Fig. 2 of Ref. 32. The last factor takes into account the reduction in final states available because of the partial occupation of the wide band. The bare mass may be put in terms of parameters already used by use of

$$m_b = \hbar^2 / 2Ja^2, \quad (15)$$

where J and a are the electronic transfer integral and lattice constant.

For given values of the degeneracy factor η , the width W_b of the wide band, the height $\delta\omega$ of the narrow band above the bottom of the wide band, and a rectangular density of states for the wide band, use of Fermi-Dirac statistics gives two relations between the carrier concentrations per Ni atom N_1 and N_2 in the narrow and wide bands and the Fermi energy E_F . For a given total carrier concentration per atom $N = N_1 + N_2$, we can thus determine N_1 , N_2 and E_F numerically. We use an iterative method for this.

Thus, for a given degeneracy factor η and given lattice

constant, we have seven parameters appearing in the expressions given above for the four contributions to the total conductivity

$$\sigma = \sigma_1 + \sigma_2 + \sigma_3 + \sigma_4 . \quad (16)$$

These parameters are the electronic transfer integral, J , the phonon energy, ω , the height δ of the narrow band above the bottom of the wide band in units of ω , the preferred numbers of phonons S_1 and S_2 to be emitted in $N \rightarrow N$ and $W \leftrightarrow N$ transitions, and the position E_0 and width Γ of the assumed Gaussian form to represent σ_4 .

Ranges of possible values for most of the parameters are known. Estimates for J may be made from bandwidths given by band-structure calculations, ω is probably bounded above by the largest phonon energy, although one cannot be completely confident of this because of possible contributions to polaron binding energies from electron-plasmon interactions or from magnetic interactions. Approximate bounds to the ratio S_2/S_1 have been obtained previously for a cubic lattice in Ref. 15. We know little about E_0 and Γ , except that they are probably bounded below by the peak position and equivalent halfwidth parameter for isolated large polarons³² (which, e.g., for $\alpha=3$ are about 2ω and 1.4ω) and, at a guess, not more than a few tenths of an eV greater than these values due to effects of disorder and Coulomb interactions. Even less is known about the parameter δ , since $\delta\omega$ is the difference between two larger quantities, i.e., the binding energies of the two types of polarons.

We assume that each excess oxygen atom produces two holes per Ni atom, and hence that

$$N_t = 0.44 \quad (17)$$

in our sample. This value is probably an upper limit, and

could be reduced by compensating hole traps. For the lattice constant we use

$$a = 2^{-1/2}(a_0 + b_0) , \quad (18)$$

where $a_0 = 5.393 \text{ \AA}$ and $b_0 = 5.446 \text{ \AA}$ are orthorhombic lattice constants at room temperature reported by Allançon *et al.*,³⁸ giving $a \approx 3.83 \text{ \AA}$. For data fitting we used a FORTRAN program which included use of a slightly modified version of a program MRQMIN from Ref. 39. We first performed fits to the data for frequencies between 1000 and 16000 cm^{-1} at six different temperatures treating all seven parameters as adjustable at each temperature, using $\eta=1$ for the degeneracy parameter; $\eta=1$ is probably the most appropriate, since there is a crystal field to separate $d_{x^2-y^2}$ and d_{z^2} orbitals,⁴⁰ although in La_2CuO_4 this splitting is only 0.4 eV.^{41,42} Our fits were made to 31 data points spaced in photon frequency by approximately 500 cm^{-1} . Possibly because of our use of theoretical expressions with discontinuous derivatives with respect to Ω at some points, which could give discontinuous derivatives with respect to some of the parameters, we found difficulty in obtaining convergence for the seven-parameter fits. However, whether or not we quite reached the minimum of our sum of squares, good fits to the data were obtained with only fairly small changes in the phonon energy, ω , between different temperatures. We continued our fitting with the value of ω fixed at 0.064 eV, the mean value from our best fits at all six temperatures from 77 to 300 K. Details of adjustable parameters and derived parameters obtained from the fits with 31 data points for $\eta=1$ are shown in Table I. The rms accuracy of the fits vary between 2.8% of the mean conductivity in the range at 300 K to 1.5% for 250 K. Uncertainties in the table would be 68% confidence levels

TABLE I. Fitting parameters to 31 points at each temperature with ω fixed at 0.064 eV, and derived quantities.

Quantity						
T (K)	77	100	150	200	250	300
Sum of squares ($\Omega^{-2} \text{cm}^{-2}$)	1584	1264	714	593	583	2737
RMS error (% of means σ)	2.7	2.6	1.9	1.8	1.5	2.8
Fitted parameters						
J (eV)	0.287 ± 0.055	0.243 ± 0.002	0.225 ± 0.001	0.222 ± 0.001	0.237 ± 0.001	0.277 ± 0.002
δ	2.81 ± 0.16	2.10 ± 0.07	2.15 ± 0.05	2.35 ± 0.04	2.71 ± 0.03	2.86 ± 0.05
S_1	32.1 ± 0.8	27.8 ± 0.2	26.1 ± 0.2	26.0 ± 0.2	26.1 ± 0.1	27.9 ± 0.2
S_2	20.2 ± 0.7	15.8 ± 0.4	14.2 ± 0.3	14.2 ± 0.2	12.66 ± 0.01	12.5 ± 0.2
E_0 (eV)	0.753 ± 0.011	0.687 ± 0.006	0.635 ± 0.004	0.575 ± 0.006	0.454 ± 0.004	0.365 ± 0.007
Γ (eV)	0.354 ± 0.012	0.348 ± 0.006	0.332 ± 0.006	0.396 ± 0.007	0.356 ± 0.004	0.297 ± 0.005
Derived quantities						
N_1	0.29	0.32	0.31	0.30	0.30	0.31
N_2	0.15	0.12	0.13	0.14	0.14	0.13
E_F (eV)	0.168	0.120	0.115	0.121	0.136	0.140
$\delta\omega$ (eV)	0.180	0.134	0.138	0.150	0.173	0.183
$S_1\omega$ (eV)	2.05	1.78	1.67	1.66	1.67	1.79
S_2/S_1	0.63	0.57	0.54	0.55	0.49	0.45
N_m^a	4×10^{-8}	4×10^{-9}	1.0×10^{-6}	3×10^{-5}	4×10^{-4}	1.3×10^{-3}
$(\omega_p \epsilon_p^{1/2})(m_{ip}/m_e)^{1/2}$ (eV) ^a	8×10^{-4}	2×10^{-4}	4×10^{-3}	0.02	0.08	0.14

^aValues for N_m and ω_p are obtained as described towards the end of Sec. V. They are at best order-of-magnitude estimates because of extra assumptions and expansion of effects of uncertainties in parameters because the parameters appear in exponents in expressions for N_m .

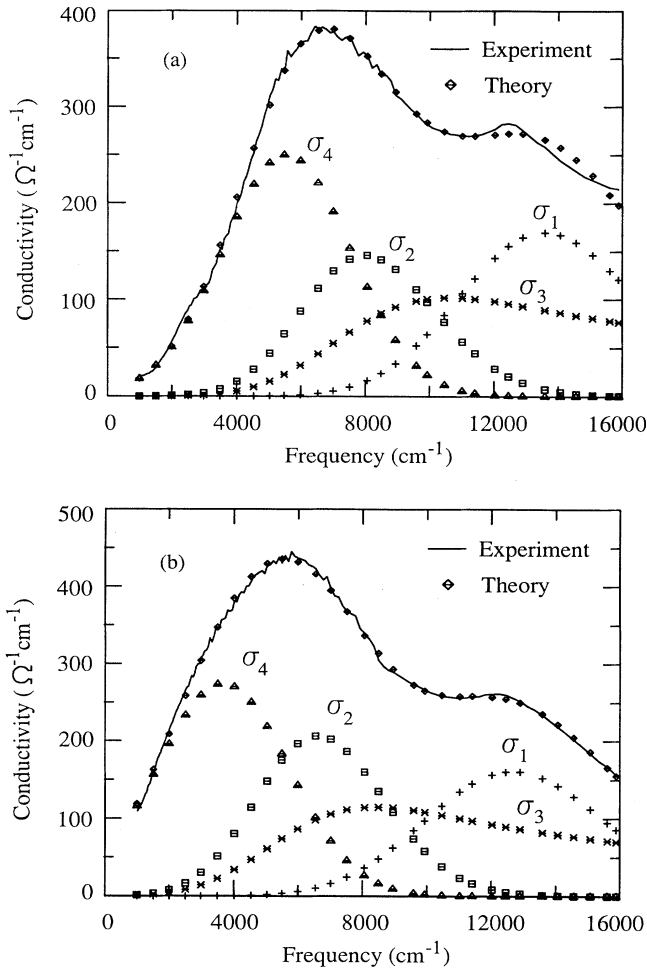


FIG. 2. Experimental and theoretical conductivity data between 1000 and 16000 cm^{-1} at two temperatures, and separation of the theoretical curves into their four components: (a) 100 K, (b) 250 K. Parameters for the theoretical curves are given in Table I.

if the theory were accurate and if experimental errors were random. If we assume that the confidence intervals should be expanded by about a factor of 5 in most cases to take into account that neither of these assumptions is likely to be correct, then the results for most temperatures are consistent with the parameters S_1 , S_2 , and Γ being independent of temperature, and with J being constant between 100 and 250 K. Comparison between theory and experiment for the temperatures 100 and 250 K together with the decomposition of the theoretical curves into their four components are shown in Figs. 2(a) and 2(b). In the model, since there are four contributions to the conductivity which peak at different energies, the observed first peak is due to combinations of contributions from σ_2 and σ_4 , with the initial states in the wide band, and the second peak or shoulder is due mainly to σ_1 , with both the initial and final states in the narrow band. Typical positions of various energy levels are shown in Fig. 3.

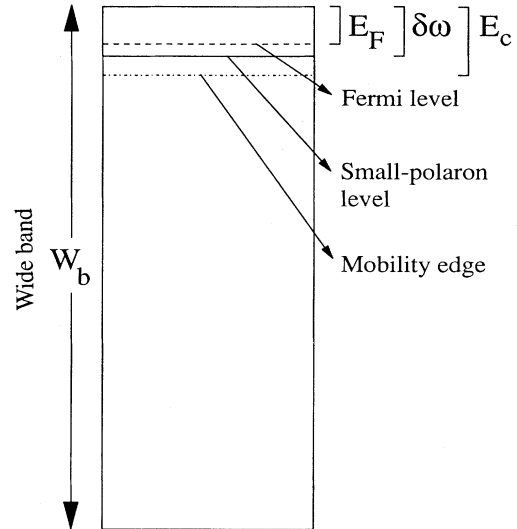


FIG. 3. Positions of energy levels for the case when current carriers are holes. Average values from fits to the data at six temperatures for W_b , $\delta\omega$, and E_F for $\text{Pr}_2\text{NiO}_{4.22}$ are, respectively, 2.0, 0.16, and 0.13 eV. In Sec. V the distance E_c of the mobility edge from the top of the wide band is estimated to be approximately 0.26 eV.

V. DISCUSSION

A. Temperature dependence of effective charges

A very useful property of a model for the dielectric function of the type described by Eq. (1) is that TO and LO frequencies can be obtained directly. Knowledge of TO-LO splitting allows us to calculate the effective charge of ions in the material by³¹

$$\sum_j (\Omega_{j\text{LO}}^2 - \Omega_{j\text{TO}}^2)_\alpha = \frac{1}{\epsilon_v V} \sum_k \frac{(Ze)_{k\alpha}^2}{m_k}, \quad (19)$$

α being a direction of polarization, m_k the mass of the k th ion, ϵ_v the vacuum permittivity and Ze_k the effective charge of the k th ion. Equation (19) together with charge neutrality $\sum_k (Ze)_{k\alpha} = 0$ for each direction gives exact results for diatomic materials. For three or more different atoms, an estimate of the effective charge of one or more atoms must be given. Anyway, as the right-hand side of Eq. (19) depends on the inverse of each ion mass, effective charges of lighter ions can be determined with great accuracy.

From phonon frequencies determined by fits to $\text{Pr}_2\text{NiO}_{4.22}$ reflectivity data in the low-frequency region shown in Fig. 1, we can obtain interesting results from effective charge calculations based on Eq. (19). Although we have three unknowns (the effective charge of each kind of atom in this material) and only two equations [Eq. (19) and charge neutrality], we can have very good estimates of the oxygen effective charge as the mass of this ion is quite smaller than the masses of the other two atoms (Pr and Ni). A completely ionic bond would yield an effective charge for a specific ion equal to its formal

valence. A covalent character of the chemical bond in the crystal diminishes this value of the effective charge. In conducting oxides, the overlap between orbitals is quite strong and thus we can expect effective charges rather smaller than formal valences. Solving the equations shows that the Pr effective charge lies between 1.0 and 1.3 (formal valence for this atom is 3). The Ni effective charge, for all temperatures, remained between 0.5 and 1 (a physically reasonable range). Error bars for the oxygen effective charge are almost negligible in comparison to the thermal variation of its value. Calculated values are shown in Fig. 4.

A clear thermally activated process is present in this material as shown by the thermal dependence of the low-frequency infrared spectra. Assuming that Pr compounds are not very different from La compounds we can expect an activation energy W for Pr_2NiO_4 of the same magnitude of La_2NiO_4 . In lanthanum compounds we have $W = 130$ meV.⁴³ Assuming that the electrons in oxygen which have the same activation energy are the two electrons needed to complete the $2p$ level we can say that the effective charge of oxygen at high temperatures is zero if all the effective charge variation is due to this activation process. Within this frame we can write the contribution of thermally activated electrons for oxygen effective charge variation as

$$Z = Z_0(1 - e^{-W/k_B T}), \quad (20)$$

where Z is the effective charge for ab plane bond, the fitting parameter Z_0 is its value at 0 K, W is the activation energy, and k_B is Boltzmann's constant.

The thermally activated contribution to the variation of Z_{oxygen} is shown as the continuous line in Fig. 4. First of all, we see that there is a variation of 10^{-3} electrons per oxygen atom between 77 K and room temperature. This variation is compatible with estimated values presented in Table I. However, we can see that the actual oxygen effective charge variation is much more important

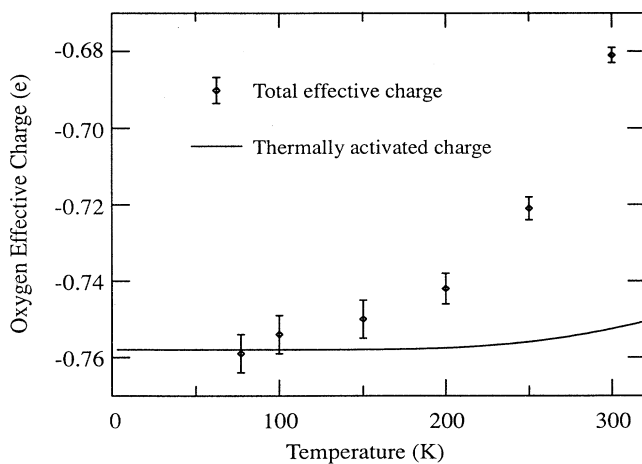


FIG. 4. Temperature dependence of ab plane oxygen effective charge (points) determined from Eq. (19) and the thermally activated contribution to it (solid line) obtained from Eq. (20).

than that predicted only by means of thermally activated processes. This difference can be explained in terms of a renormalization of the hybridization of the Ni-O bond. If at room temperature the overlapping between O and Ni orbitals is more important than at liquid-nitrogen temperature, the difference observed between the oxygen effective charge and the thermally activated contribution to this effective charge can be attributed to these changes in the Ni-O bond.

B. Polaron parameters

We next discuss the values of parameters determined by the fits to the data in the frequency range 1000 to 16 000 cm^{-1} . In this connection we first remark that our method of calculating N_2 described in Sec. IV implies neglect of (a) increases in densities of states near the bottom of the band because polaron masses are larger than bare masses, and (b) decreases in densities of states because of formation of band tails due to disorder. The neglect of these complications gives one reason for caution about the accuracy of the values of parameters found. Nevertheless, we shall find that parameter values generally lie within ranges which we expect from theoretical considerations.

First we consider values of the electronic transfer integral J . Guo and Temmerman have presented results of band-structure calculations for both paramagnetic and antiferromagnetic La_2NiO_4 .⁴⁴ From their Figs. 1 and 2 we see that two bands cross the Fermi level in both cases, and that in the paramagnetic case their widths are about 3.2 and 1.0 eV, while in the antiferromagnetic case they are about 1.9 and 1.6 eV. The average bandwidth over the six temperatures from the values of J given in Table I is about 2.0 eV, which is near the mean of the above four values. We do not know to what extent correlation affects the band-structure results in doped samples, but in the undoped case correlation has the drastic effect of making the material an insulator⁴⁵ instead of having overlapping bands as in the band-structure calculations. Since J in the oxides is indirect via oxygen, then the increases in J shown in Table I at 77 and 300 K, if real, could be related to changes in energy differences between Ni and O levels. At 77 K this could be because of effects of magnetism at this temperature.

The fact that two bands cross the Fermi level in the band-structure calculations may make it appear that a degeneracy factor $\eta = 2$ might be more appropriate than $\eta = 1$, but we have to bear in mind that, in a multiband model with on-site Coulomb repulsion, often referred to as a Hubbard model but introduced earlier by des Cloiseaux and Gutzwiller,^{46,47} there is a tendency for orbitals which have larger occupation to have this increased further relative to the other orbitals because of effects of the intrasite repulsion.⁴⁸ We did not perform fits with $\eta = 2$ with the equations given here. However, in earlier fits in which we used expressions similar to those of Ref. 15 for σ_2 , we found that the fits with $\eta = 2$ were slightly but not significantly poorer than those with $\eta = 1$. Five of the parameters for the $\eta = 2$ fits had values close to those for $\eta = 1$, while J was decreased by a factor of

about $2^{-1/2}$; values for δ were also reduced, as were the deduced values of E_F .

The largest phonon energy in Pr_2NiO_4 is 0.079 eV.²⁶ The average value which we obtained from our preliminary seven-parameter fits is 0.064 eV. An energy of about 0.064 eV is slightly higher than we would expect for a weighted average energy of various phonons. In SrTiO_3 a weighted average for long-range forces was found in Ref. 9 by methods developed earlier²⁹ to be only 0.01 eV below the maximum phonon energy. For the doped nickelates we have complications due to the presence of plasmons, and for calculations of weightings of c axis and ab plane phonons for large-polaron coupling constants, we also have the problem of an unknown mass ratio between the two directions. However, making what we hope are plausible assumptions about how to deal with the electron-plasmon interaction, one of us (D.M.E.) finds that an appropriate average energy for long-range forces for the sample of La_2NiO_4 studied in Ref. 31 seems to be closer to 0.05 eV in this sample. The slightly larger energies found from our data fitting in this paper may indicate that polaron binding energies are in part due to interaction with magnetic excitations. A similar problem was found when better fits to photoinduced absorption in semiconducting Y-Ba-Cu-O using a model involving transitions from a bound state below a small-polaron band to a small-polaron band were found for phonon energies larger than the maximum phonon energy than for the energy of the localized phonons near the photoinduced carriers.⁴⁹ In $(\text{La,Sr})_2\text{CuO}_4$ several authors think that the midinfrared absorption data might be explained without invoking electron-phonon interactions at all.⁷ Probably both correlation-induced effects and electron-phonon interactions should be included in a complete theory, but the development of such a theory in sufficient detail for accurate fitting of experimental data would be very difficult.

The product $S_1\omega$ is related to a similar quantity which would occur if J were zero, which has been called F previously,¹³⁻¹⁵ by

$$S_1\omega = F - (2zJ^2/F)(1 - \epsilon), \quad (21)$$

where ϵ is a small quantity which can be estimated from numbers given in Ref. 14 to be about 0.14 in SrTiO_3 . The average values of J and of $S_1\omega$ from numbers in Table I are about 0.25 and 1.8 eV, and so, putting $\epsilon = 0.14$ in the above equation, we find $F \approx 2.0$ eV. Further, F is related to the small-polaron binding energy which would occur in the limit $J = 0$. To connect with previous work,^{13-15,19} we call this limiting small-polaron binding energy $D\omega$. For short-range forces F is twice the $J = 0$ binding energy,⁵⁰ whereas for long-range forces it is of the order of the binding energy.¹⁵ Inclusion of effects of finite J to first and second order will change the binding energy E_b to^{13,15}

$$E_b = D\omega - zJ + zJ^2/F. \quad (22)$$

Hence, with the above figures, we deduce that E_b lies in a range between about 0.1 and 1.1 eV, the first figure being for short-range forces and the second for long-range forces. Since large-polaron binding energies are probably not greater than about 0.4 eV (e.g., for $\alpha = 5$ they are

5.44ω),⁵¹ and the values of $\delta\omega$ in Table I imply that large-polaron binding energies are at least 0.13 eV higher than binding energies of nearly small polarons at low temperatures, our values of parameters seem to imply that short-range forces are dominant. This is also implied by our larger value of $F \approx 2.0$ eV than the value of about 1.3 eV found in what was thought to be the most physical of two variants of the mixed-polaron model used in Ref. 9 to fit data in SrTiO_3 .

The average value of the ratio S_2/S_1 from Table I is 0.54. Taking, e.g., $\alpha = 4$ and $S_1 = 28$ in Eq. (36) of Ref. 15, the inequalities become $0.42 < S_2/S_1 < 0.78 + O(0.1)$, and so the empirical value of S_2/S_1 lies well within this range, but nearer to the lower limit which is expected for dominant short-range forces.

The magnitude of $\delta\omega$, the energy of the narrow band above the bottom of the wide band has been discussed above. Since this quantity depends on the difference of two polaron binding energies, neither of which are known accurately, all we can say at present is that the values are plausible.

Our best guess at the polaron coupling constant comes from the work of Ref. 17 where the range of α for which two types of polaron solution exist is shown to be between about 2.7 and 4.7 for $6J = 5\omega$ for a simple cubic lattice. From a crossover point $\alpha \approx 3$ for a smaller value of J shown in Fig. 3 of Ref. 17, we infer that, for higher values of J as obtained here, the range of α for which two solutions exist may shift to slightly higher values of α . If, e.g., $\alpha = 5$ still permits two solutions we could have a large-polaron binding energy of $5.44\omega = 0.35$ eV. Since the value of the peak in large-polaron absorption given in Ref. 32 is about $0.7\alpha\omega$, if $\alpha = 3$ or $\alpha = 5$, we deduce from the value of E_0 inferred from the data at the two lowest temperatures that disorder and Coulomb interactions increase the energy at the peak by at least 0.4 eV. Values of the halfwidth parameter are increased from that shown in Ref. 32 for $\alpha = 3$ by an average of about 0.26 eV, and from that for $\alpha = 5$ by 0.27 eV, values comparable to the low-temperature shift of the peak position. The decrease of peak position as temperature rises is probably due to the increased importance of processes in which phonons are absorbed as temperature rises, in analogy to similar effects for small-polaron theory.^{8,19}

C. Mobility edge

Since an activated conductivity is observed between 300 and 600 K for a ceramic sample of the same composition,³⁸ and our theory gives an appreciable concentration of wide-band carriers, we have to assume that the states near the bottom of this band are localized, and the activation energy involves a mobility edge. Accurate calculations of the temperature dependence of the concentration of carriers above the mobility edge in the wide band is not easy because of uncertainties in fitting parameters. However, for a first approximation, if we neglect (a) the temperature dependence of E_F between 300 and 600 K, (b) suppose that the carrier concentration above the mobility edge E_c is proportional to $T \exp[-(E_c - E_F)/k_B T]$, and (c) assume that the mobility is proportional to

$[\exp(\omega/k_B T) - 1]$, with $\omega = 0.064$ eV, we deduce from the conductivity data that $(E_c - E_F) \approx 0.12$ eV. Hence, using a value of $E_F = 0.140$ eV from Table I at 300 K, we find that $E_c \approx 0.26$ eV. These numbers may be compared with a value of about 0.2 eV from the Fermi energy inferred by Yu *et al.* from photoconductivity data on $\text{YBa}_2\text{Cu}_3\text{O}_{6.3}$.⁵² While there could, in principle, be an appreciable contribution from the narrow-band (small-polaron) carriers to the conductivity, the activation energy $(0.25S_1\omega - J)$ for (adiabatic) small-polaron hopping inferred from our analysis is about 0.20 eV, and so we think that the conductivity is dominated by the large polarons which are excited above the mobility edge.

Assuming that the value of E_c found above is independent of T and using $W_b = 2.0$ eV, we calculate from the E_F values in Table I that the concentrations N_m of mobile carriers per Ni atom are as shown in the second-to-last line of the table; values of the plasmon energies ω_p are shown on the last line in terms of the large-polaron mass, m_{lp} , and the dielectric constant, ϵ_p , appropriate for screening the plasmons. For a bare mass $m_b \approx 1.1m_e$ deducible from $J \approx 0.25$ eV and $a = 3.83$ Å, and an assumed α of between 3 and 5, we deduce from results in Ref. 51 that m_{lp}/m_e lies between 2.1 and 4.3. Also, since plasma frequencies are lower than phonon energies in most cases, ϵ_p is probably closer to the static than to the high-frequency dielectric constant. Uncertainties in E_F become magnified for calculations of carrier concentrations above E_c because of exponential factors, and so the plasma frequencies shown are probably only useful for order-of-magnitude purposes. However, it seems safe to say that the model implies very low values of plasma frequencies at temperatures below 300 K. These may be difficult to isolate directly from the experimental data.

The value of the resistivity for the polycrystalline specimen used in Ref. 38 is $0.16 \Omega \text{ cm}$ at room temperature. This value, combined with the carrier concentration given in Table I for 300 K, and the volume V_a per Ni atom³⁸ of 91.2 \AA^3 , gives a mobility $\mu = 2.7 \text{ cm}^2 \text{ V}^{-1} \text{ s}^{-1}$. From the work of Schultz,⁵¹ the mobility of large polarons near the bottom of the band for $\alpha = 3$ and $\omega = 0.064$ eV can be calculated to be $105 \text{ cm}^2 \text{ V}^{-1} \text{ s}^{-1}$. The difference by a factor of about 40 (which is only an order of magnitude estimate because of large uncertainties in N_m) can perhaps be attributed to a combination of four causes (a) reduced conductivity in polycrystalline specimens compared to that in the *ab plane* of single crystals due to effects of averaging over directions and due to effects of grain boundaries, (b) reduction of mobility because the mobile polarons are not near the bottom of the band if one includes the region of localized states, (c) larger weighting of low-energy phonons for scattering processes because of phonon-occupation factors, and (d) other scattering mechanisms than scattering by optical phonons.

D. Lack of polaron mixing

Finally we discuss the consistency of our neglect of mixing of different polaron types. An expression for the mixing matrix element is given by Eq. (36) of Ref. 14 and its value for SrTiO_3 was discussed in both Refs. 9 and 14. A prefactor in this matrix element is $-\exp[Y - (P + D)/2]$, where $D\omega$ is the small-polaron binding energy which would occur for zero J , Y is of the order of the large-polaron coupling constant, α , but rather smaller, and $P = 0.5\alpha$. We mentioned above that the value of $D\omega$ is expected to be between about F and $2F$, depending on whether long- or short-range forces dominate, where F is the value which $S_1\omega$ would take if overlap integrals were zero. Further we estimated above that $F \approx 2.0$ eV. Thus, with ω of 0.064 eV, we deduce a value for D between 16 and 32, with the high end of the range being more probable because of our inference of the dominance of short-range forces. Thus we expect that $D > 20$. Hence, with $Y < \alpha$, and $P = 0.5\alpha$, with $\alpha < 5$, we deduce that the magnitude $\exp[Y - 0.5(P + D)]$ of the prefactor in the matrix element between polaron states mentioned above is smaller than e^{-6} . Thus, since postfactors involve quantities of differing signs of the order of 1 eV,^{9,14} we deduce that matrix elements of the Hamiltonian between different types of polarons in our sample are probably considerably smaller than 0.01 eV, thus justifying the consistency with our fitting parameters of our initial assumption of negligible mixing.

VI. CONCLUSIONS

Good fits to infrared conductivity in the frequency range from 50 to $16\,000 \text{ cm}^{-1}$ have been obtained on the assumptions that (i) large and small polarons coexist in $\text{Pr}_2\text{NiO}_{4.22}$, and (ii) that phonons are screened by an overdamped plasmon in the low-frequency range. Parameter values obtained from the fits lie within ranges expected from other considerations. Short-range forces appear to give a large contribution to small-polaron binding energies. Combining values of parameters with results from Ref. 38 for conductivity permits an approximate estimate to be made of the position of the mobility edge in the large-polaron band, and order of magnitude estimates of concentrations of mobile carriers and plasma frequencies. There are both highly temperature dependent and very small below room temperature.

ACKNOWLEDGMENTS

We wish to thank the authors of Refs. 38, 42, and 43 for copies of the manuscript in advance of publication, K. Dembinski for providing the crystal, and P. Odier and J. P. Loup for helpful discussions. One of us (D.M.E.) wishes to thank the CNRS for a six-month visiting-scientist position at the CRPHT. R.P.S.M.L. acknowledges the Brazilian agency CNPq for financial support.

*Address from November 1994: Institute of Solid State Physics, Bulgarian Academy of Sciences, 72, Tzarigradsko Chaussee Blvd., 1784 Sofia, Bulgaria.

†Author to whom reprint requests should be addressed.

¹T. Timusk and D. B. Tanner, in *Physical Properties of High Temperature Superconductors*, edited by D. M. Ginsberg (World Scientific, Singapore, 1989), Vol. I, p. 338.

²See, e.g., Z. Schlesinger, R. T. Collins, F. Holtsberg, C. Feild,

- G. Koren, and A. Gupta, Phys. Rev. B **41**, 11 237 (1990).
- ³S. Y. Tian and Z. X. Zhao, Physica C **170**, 279 (1990).
- ⁴M. J. Rice and Y. R. Wang, Phys. Rev. B **36**, 8794 (1987); D. Mihailović, C. M. Foster, K. Voss, and A. J. Heeger, *ibid.* **42**, 7989 (1990).
- ⁵H. L. Dewing and E. K. H. Salje, Supercond. Sci. Tech. **5**, 50 (1992); A. S. Alexandrov, A. M. Bratkovsky, N. F. Mott, and E. K. H. Salje, Physica C **215**, 359 (1993); L. Mihailov, M. Ivanovich, and M. Georgiev, J. Phys. Soc. Jpn. **62**, 243 (1993).
- ⁶D. B. Romero, C. D. Porter, D. B. Tanner, L. Forro, D. Mandrus, L. Mihaly, G. L. Carr, and G. P. Williams, Solid State Commun. **82**, 183 (1992).
- ⁷See, e.g., J. Lorenzana and L. Yu, Phys. Rev. Lett. **70**, 861 (1993); J. A. Riera and E. Dagotto, Phys. Rev. B **50**, 452 (1994).
- ⁸H. G. Reik, Z. Phys. **203**, 346 (1967).
- ⁹D. M. Eagles and P. Lalouis, J. Phys. C **17**, 655 (1984).
- ¹⁰X.-X. Bi and P. C. Eklund, Phys. Rev. Lett. **70**, 2625 (1993).
- ¹¹X.-X. Bi, P. C. Eklund, and J. M. Honig, Phys. Rev. B **48**, 3470 (1993).
- ¹²D. A. Crandles, T. Timusk, J. D. Garret, and J. E. Greedan, Physica C **216**, 94 (1993).
- ¹³D. M. Eagles, Phys. Rev. **145**, 645 (1966).
- ¹⁴D. M. Eagles, Phys. Rev. **181**, 1278 (1969). Errors in this paper are mentioned in Sec. 4 of Ref. 9.
- ¹⁵D. M. Eagles, J. Phys. C **17**, 637 (1984). The following errors or misprints in this paper should be noted: (i) In the abstract and conclusions it was stated that both parts of the $W \rightarrow W$ contribution to the absorption fall as (photon energy) $^{-5/2}$ at high energies. This is not true for the part K_{42} of this contribution with final states in the ground mixed-polaron band; K_{42} becomes zero in the weak-coupling approximation used at photon energies $\Omega >$ (photon energy) + (energy width of the ground mixed-polaron band). (ii) Page 642. In Eq. (12) “ h ” should be “ \hbar .” In Eq. (13) “ E_{nk} ” should be “ \bar{E}_{nk} .” In Eq. (16) “ $H_i(s, n)$ ” should be “ $H_i(s, \vec{n})$.” In the line above Eq. (17) “ H_i ” is omitted immediately after the summation sign. (iii) Page 645. Seventh line after Eq. (29), “ (dE_f/dk_f) ” should be “ (dk_f/dE_f) .” (iv) Page 646. Fourth line from bottom, “photon” should be “polaron.” (v) Page 648. Third line after Eq. (38), “photon” should be “phonon.” (vi) Page 651. Fifth line from bottom $[(S_i - 3/2)\hbar\omega - \epsilon]$ should be $[(S_i - 3/2)\hbar\omega + \epsilon]$. Third line from bottom, “ $\epsilon\hbar\omega$ ” should be “ ϵ .” All of these misprints except one were noted in a footnote in Ref. 6.
- ¹⁶D. M. Eagles, in *Physics of Disordered Materials*, edited by D. Adler and H. Fritzsche (Plenum, New York, 1985), p. 357.
- ¹⁷Y. Lépine and Y. Frongillo, Phys. Rev. B **46**, 14 510 (1992).
- ¹⁸H. Fröhlich, Adv. Phys. **3**, 325 (1954).
- ¹⁹D. M. Eagles, Phys. Rev. **130**, 1381 (1963). The following errors in this paper should be noted: (i) There is a mistake in Eq. (61) due to a false method of derivation of the polaron binding energy E_b ; the factor of a half on the right-hand side should be deleted. This mistake gives an error by a factor of a half in the estimate of the polaron binding energy of NiO on p. 1396. (ii) On p. 1389 towards the end of the second column “a lattice distance” should be “an atomic distance.” (iii) The factor multiplying the integral on the right-hand side of Eq. (65) should be $(-2/\omega_{\max}G)$.
- ²⁰J. Devreese, W. Huybrechts, and L. Lemmens, Phys. Status Solidi (b) **48**, 77 (1971).
- ²¹A. S. Alexandrov, V. V. Kabanov, and D. K. Ray, Physica C **224**, 247 (1994).
- ²²J. G. Bednorz and K. A. Müller, Z. Phys. B **64**, 189 (1986).
- ²³J. L. Martínez, M. T. Fernández-Díaz, J. Rodríguez-Carvajal, and P. Odier, Phys. Rev. B **43**, 13 766 (1991).
- ²⁴A. de Andrés, J. L. Martínez, and P. Odier, Phys. Rev. B **45**, 12 821 (1992).
- ²⁵M. T. Fernández-Díaz, J. Rodríguez-Carvajal, J. L. Martínez, G. Fillion, F. Fernández, and R. Saez-Puche, Z. Phys. B **82**, 275 (1991).
- ²⁶R. P. S. M. Lobo, C. Allançon, K. Dembinski, P. Odier, and F. Gervais, Solid State Commun. **88**, 349 (1993).
- ²⁷F. Gervais, R. P. S. M. Lobo, C. Allançon, N. Pellerin, J.-M. Bassat, J.-P. Loup, and P. Odier, Solid State Commun. **88**, 245 (1993).
- ²⁸J. Yamashita and T. Kurosawa, J. Phys. Soc. Jpn. **15**, 802 (1960).
- ²⁹D. M. Eagles, J. Phys. Chem. Solids **25**, 1243 (1964). In Eq. (7) of this paper “ $\omega_{\lambda\mu}^2$ ” should be “ $\omega_{\lambda\mu}^2$ ” and in Eq. (24) a dagger is left off “ $b_{\lambda, -w}^\dagger$ ”.
- ³⁰K. Dembinski, J. M. Bassat, J. P. Coutures, and P. Odier, J. Mater. Sci. Lett. **6**, 1365 (1987).
- ³¹F. Gervais, P. Echegut, J. M. Bassat, and P. Odier, Phys. Rev. B **37**, 9364 (1988).
- ³²J. Devreese, J. de Sitter, and M. Goovaerts, Phys. Rev. B **5**, 2367 (1972).
- ³³V. V. Bryksin, Fiz. Tverd. Tela **24**, 1110 (1982) [Sov. Phys. Solid State **24**, 627 (1982)]; H. Fehske, D. Ihle, J. Loos, U. Trapper, and H. Büttner, Z. Phys. B **94**, 91 (1994).
- ³⁴F. Gervais, J.-L. Servoin, A. Baratoff, J. G. Bednorz, and G. Binnig, Phys. Rev. B **47**, 8187 (1993).
- ³⁵H. P. R. Frederikse, W. R. Thurber, and W. R. Hosler, Phys. Rev. **134**, A442 (1964); E. Ambler, J. H. Colwell, W. R. Hosler, and J. F. Schooley, Phys. Rev. **148**, 280 (1966).
- ³⁶A. H. Kahn and A. J. Leyendecker, Phys. Rev. **135**, A1321 (1964).
- ³⁷D. Emin, Phys. Rev. B **48**, 13 691 (1993).
- ³⁸C. Allançon, A. Gonthier-Vassal, J. M. Bassat, J. P. Loup, and P. Odier, Solid State Ionics **74**, 239 (1994).
- ³⁹W. H. Press, B. H. Flannery, S. A. Teukolsky, and W. T. Vetterling, *Numerical Recipes* (Cambridge University Press, Cambridge, 1986).
- ⁴⁰J. B. Goodenough and S. Ramasesha, Mater. Res. Bull. **17**, 383 (1982).
- ⁴¹J. D. Perkins, J. M. Graybeal, M. A. Kastner, R. J. Birgenau, J. P. Falck, and M. Greven, Phys. Rev. Lett. **71**, 1621 (1993).
- ⁴²J. P. Falck, J. D. Perkins, A. Levy, M. A. Kastner, J. M. Graybeal, and R. J. Birgenau, Phys. Rev. **49**, 6246 (1994).
- ⁴³J. M. Bassat, J. P. Loup, and P. Odier, J. Phys. Condens. Matter **6**, 8285 (1994).
- ⁴⁴G. Y. Guo and W. M. Temmerman, J. Phys. C **21**, L803 (1988).
- ⁴⁵M. Sayer and P. Odier, J. Solid State Chem. **67**, 26 (1987).
- ⁴⁶J. des Cloiseaux, J. Phys. Radium **20**, 606 (1959).
- ⁴⁷M. C. Gutzwiller, Phys. Rev. Lett. **10**, 159 (1963).
- ⁴⁸P. Thalmeier and L. M. Falicov, Phys. Rev. B **20**, 4637 (1979); **22**, 2456 (1980); D. M. Eagles, Z. Phys. B **45**, 197 (1982); F. López-Aguilar, and J. Costa-Quintana, J. Phys. C **19**, 2485 (1986).
- ⁴⁹D. M. Eagles, Solid State Commun. **76**, 715 (1990).
- ⁵⁰D. Emin, Adv. Phys. **24**, 305 (1975). The quantity S defined in this reference is temperature dependent, and its limit as $T \rightarrow 0$ is half as large as S as defined in Refs. 13–15 and 19.
- ⁵¹T. D. Schultz, Phys. Rev. **116**, 526 (1959).
- ⁵²G. Yu, C. H. Lee, D. Mihailović, A. J. Heeger, C. Fincher, N. Herron, and E. M. McCarron, Phys. Rev. B **48**, 7545 (1993).